Nuclear Materials and Energy 18 (2019) 245–249

Contents lists available at ScienceDirect

Nuclear Materials and Energy

journal homepage: www.elsevier.com/locate/nme

Deuterium retention in tungsten based materials for fusion applications

H. Maier[a,*], T. Schwarz-Selinger[a], R. Neu[a,b], C. Garcia-Rosales[c,d], M. Balden[a], A. Calvo[c,d], T. Dürbeck[a], A. Manhard[a], N. Ordás[c,d], T.F. Silva[a,e]

[a] Max-Planck-Institut für Plasmaphysik, Boltzmannstrasse 2, 85748 Garching, Germany
[b] Technische Universität München, Boltzmannstrasse 15, 85748 Garching, Germany
[c] Ceit-IK4, Paseo de Manuel Lardizabal 15, 20018 San Sebastian, Spain
[d] Universidad de Navarra, Tecnun, Paseo de Manuel Lardizabal 13, 20018 San Sebastian, Spain
[e] Instituto de Física da Universidade de São Paulo, Rua do Matão, trav. R 187, 05508-090 São Paulo, Brazil

ARTICLE INFO

Keywords:
Deuterium retention
Tungsten heavy alloy
Tungsten self-passivating alloy
Nuclear reaction analysis
Thermal desorption

ABSTRACT

The tungsten "heavy alloy" HPM 1850, a liquid-phase sintered composite material with two weight percent Ni and one weight percent Fe, as well as the self-passivating tungsten alloy W-10Cr-0.5Y, a high temperature oxidation resistant alloy with 10 weight percent of Cr and 0.5 weight percent of Y, were investigated with respect to their deuterium retention. The samples were deuterium loaded in an electron cyclotron resonance plasma up to a fluence of $10^{25} m^{-2}$. The deuterium retention was then investigated by Nuclear Reaction Analysis and by Thermal Desorption. In HPM 1850 the observed deuterium amount was similar to pure tungsten, however the outgassing behaviour during thermal desorption was considerably faster. In W-10Cr-0.5Y the released deuterium amount during thermal desorption was about one order of magnitude higher; by comparison of nuclear reaction analysis and thermal desorption this was attributed to deeper diffusion of deuterium into the bulk of the material.

1. Introduction

The general present-day assumption for the choice of plasma-facing materials in future fusion devices is to use tungsten for both, the divertor and the main chamber wall, see for instance [1]. These applications, however, pose very different requirements to the material properties. While a divertor target material must have sufficient toughness to withstand high thermo-mechanical loads, a main chamber plasma-facing material must protect the underlying steel structures from erosion without bearing high thermo-mechanical loads. The tritium retention in the near-surface region of the plasma-facing material, the re-emission, and the diffusion of tritium into the bulk are of importance for the tritium inventory in future fusion devices [2]. This is especially important for main chamber materials because of the large surface area of the main chamber first wall in a fusion reactor.

In the European fusion community a long-term materials development programme has been conducted in the frame of the EUROfusion Workpackage Materials, which also included the development of several tungsten-based materials for divertor as well as main chamber wall application [3,4]. With respect to the plasma-material interaction properties the fusion community can readily refer to well-reviewed data for pure tungsten [5,6]. There are, however, no data available for tungsten-based materials, which are new in the fusion community.

The purpose of this contribution is to present first data for two tungsten-based materials with respect to their deuterium retention and to compare this with a reference tungsten material. For this purpose deuterium was implanted from an electron cyclotron resonance plasma and the retention was analysed by Nuclear Reaction Analysis (NRA) and Thermal Desorption (TD). This activity was performed in the frame of the EUROfusion Workpackage Plasma-Facing Components (PFC), see for instance [7].

The materials under investigation here are a so-called tungsten heavy alloy, which could be employed as an alternative divertor target material [8], and a self-passivating tungsten alloy [9], an oxidation-resistant material, which was developed in the frame of the EUROfusion Workpackage Materials to be employed on the main chamber wall of a fusion reactor. These materials will be described in more detail in Section 2. Section 3 gives the experimental details, procedures, and results. A discussion is presented in Section 4.

2. The materials

2.1. Tungsten heavy alloy

The so-called tungsten heavy alloy is a two-phase composite

* Corresponding author.
E-mail address: hans.maier@ipp.mpg.de (H. Maier).

https://doi.org/10.1016/j.nme.2018.12.032
Received 25 July 2018; Received in revised form 14 December 2018; Accepted 27 December 2018
Available online 10 January 2019

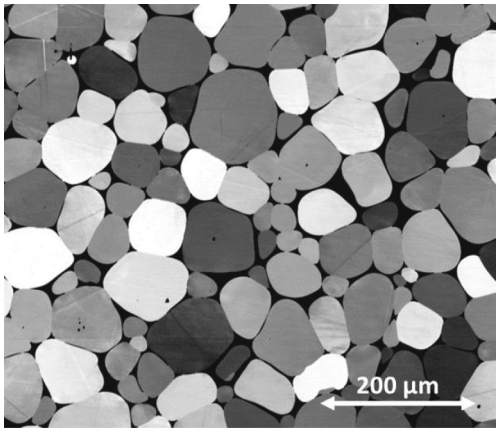

Fig. 1. SEM image of HPM 1850 in backscatter electron contrast. The different grey shades are due to grain orientation contrast; the dark area surrounding the tungsten grains is the nickel/iron matrix. The scale bar at the bottom right is 200 µm.

material consisting of tungsten powder particles in a matrix of a metal with lower melting point. It is produced by liquid phase sintering. In the original publication either copper or nickel were proposed as matrix material [10]. Here we investigate a commercially available material of tungsten with two weight percent nickel and one weight percent iron. The density of this material is 18.5 g/cm^3; it was purchased from HC Starck Hermsdorf GmbH, Germany and is labelled HPM 1850.

After a thorough pre-characterisation including high heat flux testing, which was reported in [11], this material was employed as a divertor target material in the tokamak ASDEX Upgrade. Because of its better mechanical properties the use of HPM 1850 was proposed to eliminate problems with cracking of bulk tungsten tiles, which were reported in [12]. The positive results of this measure are reported in detail in [8].

Fig. 1 shows the microstructure of HPM 1850: It consists of tungsten powder grains of sizes of a few 10 µm up to more than 100 µm surrounded by the nickel/iron matrix.

2.2. Self-passivating tungsten alloy

In the case of a loss of coolant the plasma-facing surfaces of a fusion reactor can reach high temperatures due to residual decay heat. In the European Power Plant Conceptual Studies PPCS it was shown that the outboard first wall of the reactor concepts A, B, and C can reach temperatures in excess of 1000 °C within days or tens of days [13]. Because tungsten is activated by neutron irradiation, in such a situation the ingress of oxygen would lead to the formation of volatile and radioactive WO_3, see [14] and references therein. For this reason it was proposed in [14] to use self-passivating alloys as plasma-facing materials on the first wall. In such an alloy the alloying elements form a stable oxide layer on the surface when exposed to oxygen which prevents further oxidation of the material.

The composition we investigate in this contribution consists of tungsten with 10 weight percent of chromium and 0.5 weight percent of yttrium as alloying elements, labelled W-10Cr-0.5Y. It is produced at CEIT, San Sebastian by mechanical alloying and hot isostatic pressing. Its density is 99.7% of the theoretical value from the rule of mixture. An SEM image of this material is shown in Fig. 2. The material consists of a tungsten-rich phase, which appears in light grey and a chromium-rich phase in black. The typical grain size is on the order of 100 nm. Further details can be found in [9].

2.3. Tungsten reference material

The tungsten reference material was exposed to the deuterium plasma in parallel with the respective self-passivating alloy and heavy alloy samples for comparison.

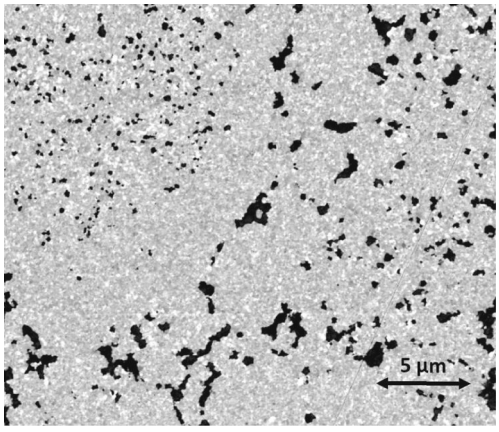

Fig. 2. SEM image of W-10Cr-0.5Y in backscatter electron contrast. The scale bar at the bottom right is 5 µm. The dark areas are a chromium-rich phase, see text.

It is a hot-rolled polycrystalline tungsten material from Plansee SE with a specified purity of 99.7%. The typical grain size is in the micrometre range, as shown in Fig. 3. A detailed microstructural analysis of this material including the effect of the applied annealing step at 930 °C can be found in [15].

3. Experimental procedures

Samples of W-10Cr-0.5Y, HPM 1850, and tungsten reference material were mechanically polished and pre-characterised by microscopy. After outgassing them in vacuum at 930 °C for one hour the samples were loaded with deuterium in an electron cyclotron resonance (ECR) plasma device. Then the deuterium retention was analysed by Nuclear Reaction Analysis (NRA) and subsequently Thermal Desorption (TD) was performed. In the following the procedures for deuterium loading as well as NRA and TD analysis are given in more detail.

3.1. Deuterium loading

Deuterium loading of the samples was performed by exposing them to a deuterium plasma from an ECR plasma source described in [16]. The plasma ions from this source are mostly D_3^+ ions. Only 3% of the impinging D flux arrives at the samples in the form of D^+ and D_2^+ ions.

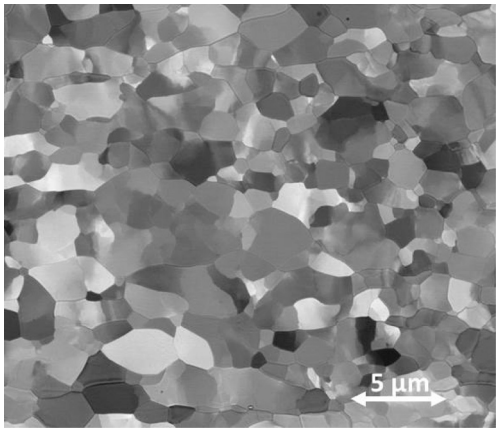

Fig. 3. SEM image of the tungsten reference material in backscatter electron contrast. The different grey shades are due to grain orientation contrast. The scale bar at the bottom right is 5 µm. The image was taken after the experiments.

D loading was performed at a sample temperature of 100 °C and a bias voltage corresponding to 38 eV/D for the D_3^+ ions. Three sets of samples were exposed to D fluences of $10^{23}m^{-2}$, $10^{24}m^{-2}$, and $10^{25}m^{-2}$, respectively. At a flux of $10^{20}m^{-2}s^{-1}$ this corresponded to exposure times of 0.3 h, 3 h, and 30 h. With each set one sample of tungsten reference material was also exposed.

3.2. Nuclear reaction analysis

Nuclear Reaction Analysis was performed using the 3 MeV tandem accelerator at the Max-Planck-Institut für Plasmaphysik in Garching.

Using the D(^{3}He,p)α reaction at ^{3}He beam energies up to 6.0 MeV and detecting the high energy protons allows probing the D content in the W samples up to a depth of approximately 10 µm. Using the software NRADC to deconvolute the proton spectra from different ^{3}He beam energies, concentration depth profiles can be constructed. In our analysis we used 6 different energies between 0.69 MeV and 6.0 MeV. NRADC is described in detail in reference [17]. It is based on a Markov chain Monte Carlo approach and is especially designed and optimised for the construction of trace element depth profiles. The software uses the SIMNRA program [18] to compute proton spectra. A subset of our data was also analysed using the independent computer code MULTISIMNRA [19]. MULTISIMNRA is a general purpose tool for analysing sets of ion beam spectra by running multiple instances of SIMNRA and performing multi-dimensional fits. The deuterium concentration depth profiles produced by using NRADC and MULTISIMNRA coincide within the error ranges given by the respective software package.

The deuterium concentration depth profiles obtained from NRADC are shown in Fig. 4. The figure contains depth profiles from 5 different samples: One tungsten reference sample (open squares), two samples HPM 1850 (open and closed triangles), two samples W-10Cr-0.5Y (open and closed circles). It can be seen that the typical deuterium concentrations are on the order of 0.1 atomic percent except in the very near surface region and deep in the bulk. Note that the concentration in the two W-10Cr-0.5Y samples remains higher than in the other samples up to the maximum information depth.

3.3. Thermal desorption

Thermal desorption was performed in the setup described in reference [20]. Basically it consists of a stainless steel vacuum vessel with a quadrupole mass spectrometer at a base pressure in the 10^{-10} mbar range. Via a metal glass transition a quartz glass tube is attached to the vessel, which contains the samples at a base pressure in the 10^{-8} mbar range. The samples can be heated up to 1050 °C by moving a tubular furnace over the quartz glass tube. In our experiments a heating ramp of 15 K/min was used.

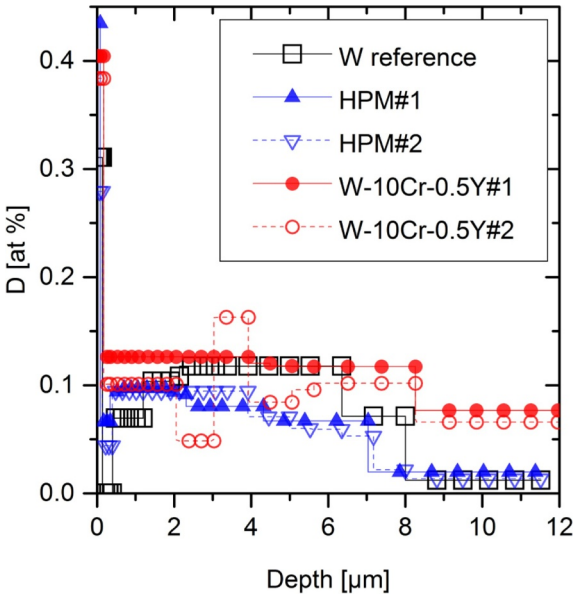

Fig. 4. Deuterium depth profiles for the samples exposed to the highest deuterium fluence of 10^{25} m^{-2} obtained by using NRADC (see text). For both, HPM 1850 and W-10Cr-0.5Y two samples each were exposed and analysed.

Fig. 5 shows D thermal desorption data for the five samples exposed to the highest implantation fluence of $10^{25}m^{-2}$: One tungsten reference sample (open squares), two samples HPM 1850 (open and closed triangles), and two samples W-10Cr-0.5Y (open and closed circles). The data from the W-1Cr-0.5Y samples are scaled down by a factor of 10.

For the pure tungsten reference samples the temperature was ramped up to 1050 °C. For the alloys the heating ramp was stopped at 850 °C. This was done because of the higher vapour pressures of the alloying metals as compared to that of pure tungsten. The mass-4 signal of the mass spectrometer when detecting D_2 gas is calibrated by injecting a calibrated flux of deuterium gas into the vessel. For deuterium arriving at the mass spectrometer in the form of HD molecules a calibration using a calibrated volume and a spinning rotor pressure gauge was used as explained in reference [21]. A part of the released deuterium, however, arrives at the mass spectrometer in the form of water HDO or D_2O, respectively, i.e. at the masses 19 and 20. For these a direct calibration factor is not available. In our measurements the relative amount of deuterium released in the form of water decreases substantially with increasing implantation fluence. Assuming the same sensitivity of the setup for HDO and D_2O as for the HD signal from mass 3, we estimate it to range from about 20–35% at the lowest applied implantation fluence to 4–7% at the highest fluence, depending on the respective material. For the HD signal the corresponding fractions vary from 15–20% to 2–12%.

4. Results and discussion

Fig. 6 shows integrated thermal desorption data for all samples investigated in this contribution. In these datasets the mass spectrometer signals for all masses discussed in Section 3.3 are included, i.e. D_2, HD, HDO, and D_2O.

The figure summarises the main result of this work: In W-10Cr-0.5Y the total deuterium content is higher than in the tungsten reference material by one order of magnitude for all employed implantation fluences. When we compare the tungsten reference material with HPM 1850, the deuterium content is of similar order. However, a fluence dependent trend is visible.

In the following the results are discussed in more detail.

4.1. HPM 1850

As Fig. 5 shows, for both HPM 1850 samples the deuterium release occurred at lower temperatures than for the tungsten reference sample. This indicates either a faster out-diffusion or lower trap binding energies in the HPM 1850 material as compared to the reference tungsten material. Another explanation would be the accumulation of deuterium closer to the surface in HPM 1850, which would represent a shorter diffusion distance. This can, however, be ruled out by comparing the measured NRA deuterium depth profiles from Fig. 4.

In reference [22] hydrogen diffusion coefficients for the pure metals nickel and iron are given. According to this reference the activation energy for hydrogen diffusion in nickel is very similar to the tungsten case, i.e. about 0.4 eV, while in iron the activation energy is significantly lower. Reference [23] shows in detail that the activation energy for hydrogen diffusion in Ni/Fe alloys actually is a function of the alloy composition and depends on the thermal history of the sample. Depending on the heat treatment, which was also performed in our case, the activation energy for hydrogen diffusion in Ni/Fe alloys can have a minimum of less than 0.2 eV in the compositional range of

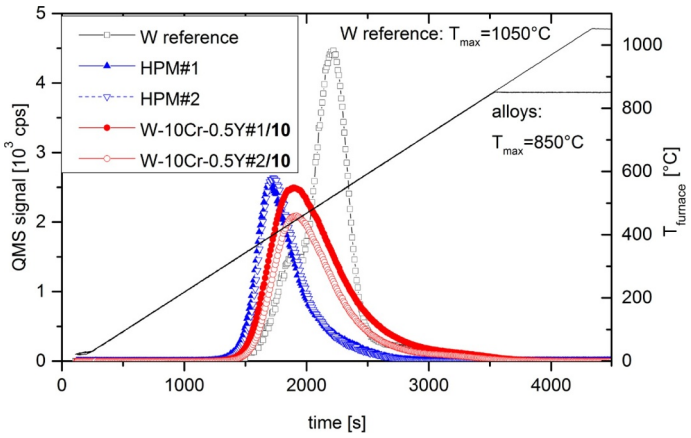

Fig. 5. D_2 thermal desorption data for the samples exposed to the highest fluence of 10^{25} m^{-2}. As in Fig. 4 two samples each were exposed and analysed for HPM1850 and W-10Cr-0.5Y. The W-10Cr-0.5Y data are scaled down by a factor of 10.

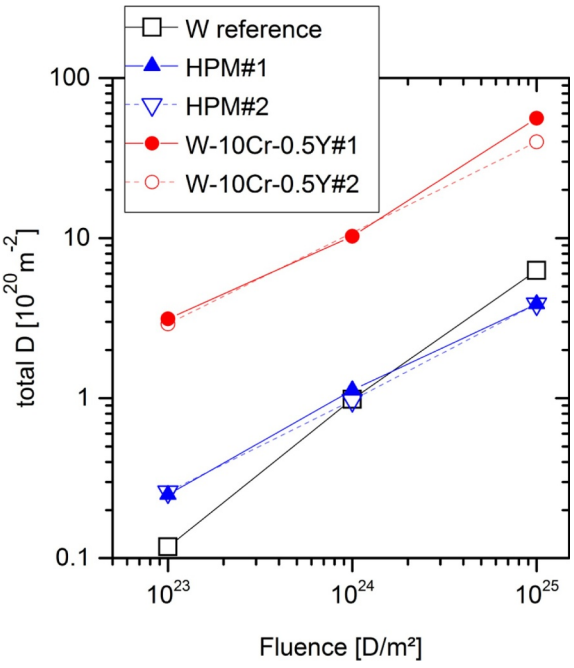

Fig. 6. Total released D amounts as a function of implantation fluence for all three materials. For HPM 1850 two samples were employed for each fluence; for W-10Cr-0.5Y two samples were employed for the highest and lowest fluence, but only one for the intermediate fluence of 10^{24} m^{-2}.

70% to 80% Ni. As this is close to the composition of the matrix material in HPM 1850, this could be the reason why the out-diffusion occurs considerably faster during the temperature ramp in the desorption experiment. However, this would only hold for hydrogen atoms diffusing in the Ni/Fe matrix.

Reference [24] gives enthalpies of solution for hydrogen in pure nickel or pure iron which are considerably lower than that of tungsten. Data on the enthalpy of solution of deuterium in a Ni/Fe alloy with the actual composition of our sample material are not available. However, if we assume the trend given for the pure materials to hold also for the alloy, then this would additionally support the faster out-diffusion process, because hydrogen atoms would energetically prefer the Ni/Fe matrix from the tungsten grains.

In summary this would mean that hydrogen atoms entering the matrix material would stay in there and leave the sample in a faster diffusion process compared to tungsten.

4.2. W-10Cr-0.5Y

Fig. 6 shows the total released amounts of deuterium. For the W-10Cr-0.5Y samples we have 2 data points for the highest and lowest deuterium implantation fluence at $10^{23}m^{-2}$ and $10^{25}m^{-2}$, and only one data point at the intermediate fluence of $10^{24}m^{-2}$.

The figure clearly shows that the amount of deuterium released by the W-10Cr-0.5Y alloy is roughly an order of magnitude higher than the corresponding amount from the tungsten reference material. This observation holds for the whole investigated implantation fluence range, which spans 2 orders of magnitude, and shows to be well reproducible in the cases where two samples per fluence were employed.

In Fig. 7 a comparison of TD data from Fig. 6 with the corresponding NRA data from the same samples is shown: As in Fig. 6 the TD data from the W-10Cr-0.5Y samples are represented by closed and open circles and the TD data from the tungsten reference samples are represented by open squares. For all samples the NRA data were obtained several days before outgassing the samples in the TD setup. They are shown as asterisks for both sample types. The comparison shows that with increasing implantation fluence the integrals of the TD data increase systematically, while the integrated NRA data stay approximately constant for the two higher fluences of $10^{24}m^{-2}$ and $10^{25}m^{-2}$. At the highest fluence the deuterium released during TD is about one order of magnitude more than the amount detected in NRA. In contrast to this, for the tungsten reference material the TD data and the NRA data for the two higher fluences coincide approximately. There is a discrepancy for the lowest fluence – here the NRA data point is higher.

In our interpretation this comparison shows that with increasing fluence, which corresponds to increasing implantation time, in the case of W-10Cr0.5-Y the implanted deuterium diffuses deeper into the material, such that at the two longer implantation times in our experiment most of the deuterium already diffused beyond the information depth of our NRA depth profiling measurements, which is about 10 µm. Therefore the TD analysis shows a larger amount of deuterium, which cannot be detected by the NRA measurements, since it is mostly trapped beyond the NRA information depth. This interpretation is supported by the fact that in Fig. 4 the deuterium concentration remains high in the maximum information depth, different from the other two materials. A possible reason for this behaviour could be the presence of a metal oxide diffusion barrier on the surface hindering the reemission of implanted deuterium.

With respect to the total retention a similar observation was made in a different tungsten alloy: In reference [25] it was observed that alloying of tungsten with 1% or 5% of tantalum, respectively, led to an increase of the retained amount of deuterium by roughly one order of magnitude for implantation fluences in the range of $10^{24}m^{-2}$, which is

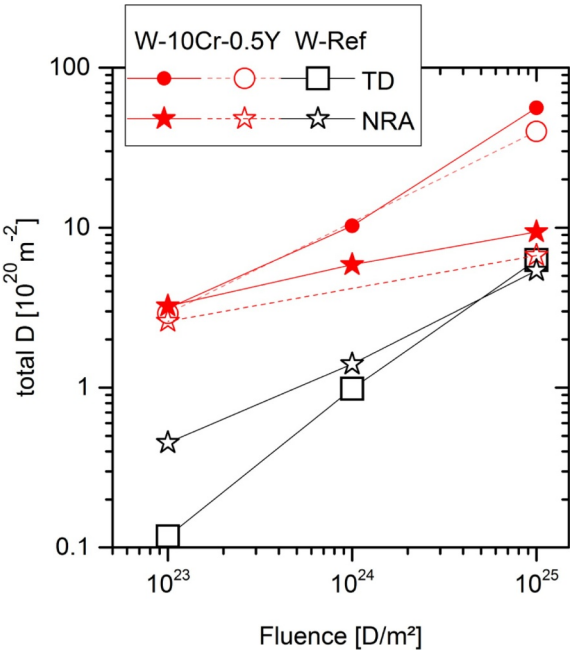

Fig. 7. Comparison of deuterium amounts for W-10Cr-0.5Y and the W reference samples. The squares and circles represent integrals from the thermal desorption data, the asterisks represent integrals obtained from the deuterium depth profiles shown in Fig. 4. The TD data are the same as in Fig. 6.

similar to the fluence range investigated here. Different from our interpretation presented here, the authors of [25] conclude from a comparison of their results with modelling, that the increased retention is due to an increase of the trap density in the material caused by tantalum alloying rather than due to deeper diffusion.

5. Summary, conclusions, and outlook

We performed an investigation of the deuterium retention in two materials, which are new in the fusion community: the tungsten heavy alloy HPM 1850, which is a liquid phase sintered material of tungsten with 3 weight percent of nickel and iron and a self-passivating alloy of tungsten with 10 weight percent of chromium and 0.5 weight percent of yttrium, W-10Cr-0.5Y, which is a material resistant to high temperature oxidation.

Samples were loaded with deuterium from an ECR plasma at 100°C with fluences of $10^{23}m^{-2}$, $10^{24}m^{-2}$, and $10^{25}m^{-2}$, respectively. These samples were then analysed with Nuclear Reaction Analysis with a ^{3}He beam of energies in between 0.69 MeV and 6.0 MeV, which allows deuterium depth profiling up to a depth of about 10 µm. Subsequently the samples were outgassed in a Thermal Desorption setup. These results were compared to results from a pure tungsten reference material.

It was found that the amount of deuterium released from HPM 1850 samples is very similar to that from pure tungsten, whereas the outgassing occurs faster during the thermal desorption temperature ramp. This was interpreted in terms of faster out-diffusion of deuterium through the Ni/Fe matrix transport channel.

For the W-10Cr-0.5Y material it was found that the amount of deuterium released during the thermal desorption temperature ramp is about one order of magnitude higher than the corresponding amount from our reference tungsten material. This is valid for all investigated implantation fluences. By comparing this result with the corresponding result from Nuclear Reaction Analysis depth profiling it was concluded that this observation is due to deeper diffusion of deuterium beyond the information depth of the ion beam analysis into the bulk of the samples.

For both sample materials investigated in this contribution our interpretation of the different behaviour when compared to our reference tungsten material involves diffusion. Therefore the next step will be the investigation of the temperature dependence of the deuterium retention. This will shed more light onto the question whether the diffusion coefficients in the W-10Cr-0.5Y alloy in one case and in the Ni/Fe matrix of HPM 1850 in the other are responsible for the observed differences.

The final step of this work will be the investigation of deuterium retention in samples irradiated with high energy ions. This allows the simulation of neutron induced radiation damage by using an MeV accelerator. In the process of the European fusion roadmap the European materials assessment group called the lack of data on the effect of irradiation on the tritium retention of tungsten materials a “highest impact project level risk” for DEMO [26].

Acknowledgement

This work has been carried out within the framework of the EUROfusion Consortium under EUROfusion WP PFC and has received funding from the Euratom research and training programme 2014–2018 under grant agreement No 633053. The views and opinions expressed herein do not necessarily reflect those of the European Commission.

References

[1] C. Bachmann, et al., Fus. Eng. Des. 112 (2016) 527.
[2] Y. Fukai, The Metal-Hydrogen System, 2nd edition, Springer, Berlin, 2005 chapter 5.
[3] M. Rieth, et al., J. Nucl. Mater. 417 (2011) 463.
[4] M. Rieth, et al., J. Nucl. Mater. 432 (2013) 482.
[5] R. Causey, J. Nucl. Mater. 300 (2002) 91.
[6] Ch. Skinner, et al., Fus. Sci. Technol. 54 (2008) 891.
[7] S. Bresinzek, et al., Nucl. Fus. 57 (2017) 116150.
[8] R. Neu, et al., J. Nucl. Mater. 511 (2018) 567.
[9] A. Calvo, et al., Int. J. Refract. Met. Hard Mater. 73 (2018) 29.
[10] C.J. Smithells, Nature 139 (1937) 490.
[11] R. Neu, et al., Fus. Eng. Des. 124 (2017) 450.
[12] A. Hermann, et al., Nucl. Mater. Energy 12 (2017) 205.
[13] D. Maisonnier, et al., Fus. Eng. Des. 75 (2005) 1173.
[14] F. Koch, H. Bolt, Phys. Scripta T. 128 (2007) 100.
[15] A. Manhard, et al., Pract. Metallogr. 52 (2015) 437.
[16] A. Manhard, et al., Plasma Sources Sci. Technol. 20 (2011) 015010.
[17] K. Schmid, U. von Toussaint, Nucl. Instr. Meth. B 281 (2012) 64.
[18] M. Mayer, SIMNRA User's Guide, Report IPP 9/113, Max-Planck-Institut für Plasmaphysik, Garching, Germany, 1997.
[19] T.F. Silva, et al., Nucl. Instr. Meth. B 371 (2016) 86.
[20] E. Saloncon, et al., J. Nucl. Mater. 376 (2008) 160.
[21] P. Wang, et al., Nucl. Instr. Meth. B 300 (2013) 54.
[22] J. Völkl, G. Alefeld, Hydrogen in Metals I, Topics in Applied Physics 28, in: G. Alefeld, J. Völkl (Eds.), Springer, Berlin, 1978chapter 12.
[23] R. Dus, M. Smialowski, Acta Metallurgica 15, 1967, 1611; see also, in: D.J. Fisher (Ed.), Hydrogen Diffusion in Metals-A 30-Year Retrospective, Scitec Publications Ltd., Zurich, 1999.
[24] E. Fromm, G. Hörz, Int. Metals Rev. 25 (1980) 269.
[25] K. Schmid, et al., J. Nucl. Mater. 426 (2012) 247.
[26] D. Stork, et al., J. Nucl. Mater. 455 (2014) 277.